

Thermalization of quark-gluon matter with the elastic scattering of gqq , $gq\bar{q}$ and $g\bar{q}\bar{q}$

Xiao-Ming Xu¹ and Li-Sha Xu²

¹ Department of Physics, Shanghai University, Baoshan, Shanghai 200444, China

² Department of Information Engineering, China Jiliang University, Hangzhou 310018, China

E-mail: xmxu@xmxucao.sina.net

Abstract. The elastic scattering of gqq , $gq\bar{q}$ and $g\bar{q}\bar{q}$ and the thermalization of quark-gluon matter are studied. According to Feynman diagrams at the tree level, squared amplitudes for the elastic gqq scattering and the elastic $gq\bar{q}$ scattering are derived in perturbative QCD. Transport equations including the squared amplitudes for the elastic gqq , $gq\bar{q}$ and $g\bar{q}\bar{q}$ scattering are established. Corresponding to anisotropic gluon and quark distributions created in central Au-Au collisions at RHIC, solutions of the transport equations show that thermalization time of quark matter can be shortened by the elastic gqq , $gq\bar{q}$ and $g\bar{q}\bar{q}$ scattering.

PACS numbers: 24.85.+p;12.38.Mh;12.38.Bx;25.75.Nq

1. Introduction

Scattering takes place in quark-gluon matter that is created in high-energy heavy-ion collisions. If quark-gluon matter has a low number density, two-body scattering substantially affects the evolution of quark-gluon matter. The two-body scattering includes the 2-to-2 scattering and the 2-to-3 scattering [1, 2, 3, 4, 5, 6, 7]. If the number density is high, the three-body scattering becomes important. This has been shown by the elastic gluon-gluon-gluon scattering in gluon matter which has a number density of the order of 19 fm^{-3} that is reached in central Au-Au collisions at the Relativistic Heavy Ion Collider (RHIC) [8]. One effect derived from the elastic gluon-gluon-gluon scattering is on the rapid thermalization of gluon matter. The elastic 3-to-3 scattering of a heavy quark contributes significantly to the heavy quark momentum degradation in the quark-gluon plasma [9]. Since at the Large Hadron Collider (LHC) Pb-Pb collisions will be carried out to produce quark-gluon matter which has a higher number density than matter reached at RHIC, the elastic 3-to-3 scattering is more involved. Therefore, we must study the elastic 3-to-3 scattering and its effects. Due to the complication of the study [10], in this work we are restricted to the elastic gluon-quark-quark scattering, the elastic gluon-quark-antiquark scattering and the elastic gluon-antiquark-antiquark scattering, and apply the scattering to thermalization of quark-gluon matter.

We display Feynman diagrams at the tree level for the elastic gluon-quark-quark scattering in Section 2 and the elastic gluon-quark-antiquark scattering in Section 3. In Section 4, as two examples, we show squared amplitudes for a diagram of the elastic gqq scattering and for a diagram of the elastic $gq\bar{q}$ scattering, respectively. We present transport equations that include the elastic scattering of gqq , $gq\bar{q}$ and $g\bar{q}\bar{q}$. In Section 5 numerical solutions of the transport equations and relevant discussions are given. The last section contains the summary.

2. Elastic gluon-quark-quark scattering

Some Feynman diagrams for the elastic gluon-quark-quark scattering are shown in Figs. 1-4. The wiggly lines and solid lines stand for gluons and quarks, respectively. The other Feynman diagrams are derived from the diagrams in Figs. 1-4 as follows.

The six diagrams in Fig. 1 lead to six new diagrams by moving the external gluons from the left quark line to the right quark line, i.e. by moving the initial gluon from an initial (final) quark to another initial (final) quark and moving the final gluon in the same way. If the two final quarks are identical, the exchange of the final quarks in the above twelve diagrams leads to twelve more diagrams. We can thus derive 18 diagrams from the six diagrams in Fig. 1.

The four diagrams in Fig. 2 lead to four new diagrams by moving the initial gluon from the initial (final) state of a quark to the final (initial) state of the same quark and moving the final gluon in the same way. If the two final quarks are identical, the exchange of the final quarks in the above eight diagrams leads to eight more diagrams. We can thus derive 12 diagrams from the four diagrams in Fig. 2.

For the elastic scattering of one gluon and two identical quarks, we need to take into account 40 diagrams that do not contain any triple-gluon vertex. Each of the 40 diagrams contains one gluon propagator and four gluon-quark vertices. The 40 diagrams form the first class of processes for the elastic gqq scattering.

Every diagram in Fig. 3 contains one triple-gluon vertex. We can derive 18 diagrams from the six diagrams. Each of the diagrams D_{-M} and D_{+M} contains one gluon propagator between the triple-gluon vertex and the left quark. The diagrams D_{-M} and D_{+M} lead to two new diagrams by letting the gluon propagating from the triple-gluon vertex to the right quark. The diagrams D_{GUML} , D_{GUMH} , D_{GDMH} and D_{GDML} lead to four new diagrams by moving the initial or final gluon from the left quark to the right quark. If the two final quarks are identical, the exchange of the final quarks in the above twelve diagrams generates twelve more diagrams.

While one triple-gluon vertex is involved in the elastic scattering of one gluon and two identical quarks, twenty-four diagrams need to be taken into consideration. Each of the 24 diagrams contains two gluon propagators and three gluon-quark vertices. The 24 diagrams form the second class of processes for the elastic gqq scattering.

The four diagrams in Fig. 4 are characterized by two triple-gluon vertices or one four-gluon vertex, and give rise to four more diagrams by the exchange of the two

final quarks if the quarks are identical. The eight diagrams contain three or two gluon propagators and two gluon-quark vertices. The 8 diagrams form the third class of processes for the elastic gqq scattering.

We have arrived at the three classes of processes represented by the 72 diagrams for the elastic scattering of one gluon and two identical quarks. If the two quarks do not possess the same flavor, the processes with the exchange of final quarks do not happen and thirty-six diagrams are needed. To ensure gauge invariance we include elastic ghost-quark-quark scattering for which some Feynman diagrams are shown in Fig. 5. Ghosts are indicated by the dashed lines. Each of the diagrams D_{-MFP} and D_{+MFP} contains one gluon propagator between the ghost line and the left quark line. If the gluon propagator is connected to the right quark line, two new diagrams are generated by the diagrams D_{-MFP} and D_{+MFP} . In total, we need 7 diagrams for distinguishable quarks and 14 diagrams for indistinguishable quarks.

3. Elastic gluon-quark-antiquark scattering

Since quark-antiquark annihilation may happen in elastic gluon-quark-antiquark scattering, the scattering involves more Feynman diagrams than the elastic gluon-quark-quark scattering. We only display some diagrams in Figs. 6-12, but the other diagrams can be derived as follows.

In each of the six diagrams in Fig. 6 the initial and final gluons are attached to the quark line. While the initial and final gluons are attached to the antiquark line, six new diagrams are produced. The four diagrams in Fig. 7 lead to four new diagrams by moving an external gluon from the final quark to the initial quark and moving another external gluon from the initial (final) antiquark to the final (initial) antiquark. Hence, there are twenty diagrams of which any contains no self-coupling of gluons and no quark-antiquark annihilation.

The external gluons in Fig. 8 are attached to one or two of the quark lines. Similarly, the initial and final gluons can be attached to one or two of the antiquark lines and six new diagrams are thus created. In Fig. 9 the four diagrams lead to four new diagrams by moving one external gluon from the final quark to the initial quark and moving another external gluon from the initial (final) antiquark to the final (initial) antiquark. Therefore, twenty diagrams exist in the case of quark-antiquark annihilation and no self-coupling of gluons.

In total, from Figs. 6-9 we have 40 diagrams of which each contains no triple-gluon coupling and no four-gluon coupling. The 40 diagrams form the first class of processes for the elastic $gq\bar{q}$ scattering.

Each of the diagrams E_{-M} and E_{+M} in Fig. 10 contains one gluon propagator between the triple-gluon vertex and the quark line. The two diagrams generate two new diagrams while the gluon propagator is connected to the antiquark line. The diagrams E_{GUML} , E_{GUMH} , E_{GDML} and E_{GDMH} generate four new diagrams while the external gluon irrelevant to the triple-gluon vertex is moved to the antiquark line. Therefore, twelve

diagrams correspond to the case in which every diagram has one triple-gluon vertex and quark-antiquark annihilation and creation do not take place.

The diagram E_{QD} (E_{QU}) in Fig. 11 contains one gluon propagator between the triple-gluon vertex and the initial (final) quark. The diagrams E_{QD} and E_{QU} give rise to two new diagrams while the gluon propagates between the triple-gluon vertex and the initial or final antiquark. In the diagram E_{QDE} the initial quark radiates a gluon that creates a quark-antiquark pair. The diagram E_{QDE} generates one new diagram by moving the gluon to the initial antiquark. In the diagram E_{QUE} the initial quark-antiquark pair annihilates into a gluon that is absorbed by the final quark. The diagram E_{QUE} generates one new diagram by moving the gluon to the final antiquark. Four new diagrams are given by the diagrams E_{GUMLA} , E_{GUMHA} , E_{GDMHA} and E_{GDMLA} by moving the external gluon irrelevant to the triple-gluon vertex from a quark to an antiquark. Finally, sixteen diagrams correspond to the case in which every diagram has one triple-gluon vertex and possesses quark-antiquark annihilation and creation.

In total, from Figs. 10 and 11 we have 28 diagrams of which each contains one triple-gluon coupling. The 28 diagrams form the second class of processes for the elastic $gq\bar{q}$ scattering.

Any of the diagrams in Fig. 12 has two triple-gluon couplings or one four-gluon coupling. The 8 diagrams form the third class of processes for the elastic $gq\bar{q}$ scattering.

We have arrived at the three classes of processes shown by the 76 diagrams. If the quark-antiquark annihilation may happen, all the 76 diagrams must be considered. If the annihilation does not occur, thirty-six diagrams are needed. To satisfy gauge invariance we include elastic ghost-quark-antiquark scattering. Some Feynman diagrams for the scattering are plotted in Figs. 13 and 14. In Fig. 13 each of the diagrams $E_{-\text{MFP}}$, $E_{+\text{MFP}}$, E_{QDFP} and E_{QUFP} has one gluon propagator between the ghost line and the quark line. If the gluon propagator is between the ghost line and the antiquark line, four new diagrams are obtained from the diagrams $E_{-\text{MFP}}$, $E_{+\text{MFP}}$, E_{QDFP} and E_{QUFP} . In the diagram E_{QDEFP} the gluon radiated from the initial quark breaks into a quark-antiquark pair. If the gluon is radiated from the initial antiquark, one new diagram is generated from the diagram E_{QDEFP} . In the diagram E_{QUEFP} the gluon from the annihilation of a quark-antiquark pair is absorbed by the final quark. If the gluon is absorbed by the final antiquark, a new diagram is generated from the diagram E_{QUEFP} . Finally, we have 6 diagrams derived from the six diagrams in Fig. 13 and together with the six diagrams in Fig. 14 we need to consider 18 diagrams for the elastic ghost-quark-antiquark scattering.

4. Transport equations

We establish transport equations for quark-gluon matter which consists of gluons, quarks and antiquarks with up and down flavors. Denote the gluon distribution function by f_{gi} where i labels the i th gluon in scattering. Let the distribution functions for the up quark, the down quark, the up antiquark and the down antiquark be f_{ui} , f_{di} , $f_{\bar{u}i}$ and

$f_{\bar{d}i}$, respectively, and we assume that they are identical,

$$f_{ui} = f_{di} = f_{\bar{u}i} = f_{\bar{d}i} = f_{qi}, \quad (1)$$

where i labels the i th quark or antiquark in scattering. With elastic 2-to-2 scattering and elastic 3-to-3 scattering, the transport equation for gluons is

$$\begin{aligned} & \frac{\partial f_{g1}}{\partial t} + \vec{v}_1 \cdot \vec{\nabla}_{\vec{r}} f_{g1} \\ &= -\frac{1}{2E_1} \int \frac{d^3 p_2}{(2\pi)^3 2E_2} \frac{d^3 p_3}{(2\pi)^3 2E_3} \frac{d^3 p_4}{(2\pi)^3 2E_4} (2\pi)^4 \delta^4(p_1 + p_2 - p_3 - p_4) \\ & \quad \times \left\{ \frac{g_G}{2} |\mathcal{M}_{gg \rightarrow gg}|^2 [f_{g1} f_{g2} (1 + f_{g3})(1 + f_{g4}) - f_{g3} f_{g4} (1 + f_{g1})(1 + f_{g2})] \right. \\ & \quad + g_Q (|\mathcal{M}_{gu \rightarrow gu}|^2 + |\mathcal{M}_{gd \rightarrow gd}|^2 + |\mathcal{M}_{g\bar{u} \rightarrow g\bar{u}}|^2 + |\mathcal{M}_{g\bar{d} \rightarrow g\bar{d}}|^2) \\ & \quad \times [f_{g1} f_{q2} (1 + f_{g3})(1 - f_{q4}) - f_{g3} f_{q4} (1 + f_{g1})(1 - f_{q2})] \left. \right\} \\ & - \frac{1}{2E_1} \int \frac{d^3 p_2}{(2\pi)^3 2E_2} \frac{d^3 p_3}{(2\pi)^3 2E_3} \frac{d^3 p_4}{(2\pi)^3 2E_4} \frac{d^3 p_5}{(2\pi)^3 2E_5} \frac{d^3 p_6}{(2\pi)^3 2E_6} \\ & \quad \times (2\pi)^4 \delta^4(p_1 + p_2 + p_3 - p_4 - p_5 - p_6) \left\{ \frac{g_G^2}{12} |\mathcal{M}_{ggg \rightarrow ggg}|^2 \right. \\ & \quad \times [f_{g1} f_{g2} f_{g3} (1 + f_{g4})(1 + f_{g5})(1 + f_{g6}) - f_{g4} f_{g5} f_{g6} (1 + f_{g1})(1 + f_{g2})(1 + f_{g3})] \\ & \quad + \frac{g_G g_Q}{2} (|\mathcal{M}_{ggu \rightarrow ggu}|^2 + |\mathcal{M}_{ggd \rightarrow ggd}|^2 + |\mathcal{M}_{gg\bar{u} \rightarrow gg\bar{u}}|^2 + |\mathcal{M}_{gg\bar{d} \rightarrow gg\bar{d}}|^2) \\ & \quad \times [f_{g1} f_{g2} f_{q3} (1 + f_{g4})(1 + f_{g5})(1 - f_{q6}) - f_{g4} f_{g5} f_{q6} (1 + f_{g1})(1 + f_{g2})(1 - f_{q3})] \\ & \quad + g_Q^2 \left[\frac{1}{4} |\mathcal{M}_{guu \rightarrow guu}|^2 + \frac{1}{2} (|\mathcal{M}_{gud \rightarrow gud}|^2 + |\mathcal{M}_{gdu \rightarrow gdu}|^2) + \frac{1}{4} |\mathcal{M}_{gdd \rightarrow gdd}|^2 \right. \\ & \quad + |\mathcal{M}_{g\bar{u}\bar{u} \rightarrow g\bar{u}\bar{u}}|^2 + |\mathcal{M}_{g\bar{u}\bar{d} \rightarrow g\bar{u}\bar{d}}|^2 + |\mathcal{M}_{g\bar{d}\bar{u} \rightarrow g\bar{d}\bar{u}}|^2 + |\mathcal{M}_{g\bar{d}\bar{d} \rightarrow g\bar{d}\bar{d}}|^2 \\ & \quad \left. + \frac{1}{4} |\mathcal{M}_{g\bar{u}\bar{u} \rightarrow g\bar{u}\bar{u}}|^2 + \frac{1}{2} (|\mathcal{M}_{g\bar{u}\bar{d} \rightarrow g\bar{u}\bar{d}}|^2 + |\mathcal{M}_{g\bar{d}\bar{u} \rightarrow g\bar{d}\bar{u}}|^2) + \frac{1}{4} |\mathcal{M}_{g\bar{d}\bar{d} \rightarrow g\bar{d}\bar{d}}|^2 \right] \\ & \quad \times [f_{g1} f_{q2} f_{q3} (1 + f_{g4})(1 - f_{q5})(1 - f_{q6}) - f_{g4} f_{q5} f_{q6} (1 + f_{g1})(1 - f_{q2})(1 - f_{q3})] \left. \right\}, \end{aligned} \quad (2)$$

and the transport equation for up quarks is

$$\begin{aligned} & \frac{\partial f_{q1}}{\partial t} + \vec{v}_1 \cdot \vec{\nabla}_{\vec{r}} f_{q1} \\ &= -\frac{1}{2E_1} \int \frac{d^3 p_2}{(2\pi)^3 2E_2} \frac{d^3 p_3}{(2\pi)^3 2E_3} \frac{d^3 p_4}{(2\pi)^3 2E_4} (2\pi)^4 \delta^4(p_1 + p_2 - p_3 - p_4) \\ & \quad \times \left\{ g_G |\mathcal{M}_{ug \rightarrow ug}|^2 [f_{q1} f_{g2} (1 - f_{q3})(1 + f_{g4}) - f_{q3} f_{g4} (1 - f_{q1})(1 + f_{g2})] \right. \\ & \quad + g_Q \left(\frac{1}{2} |\mathcal{M}_{uu \rightarrow uu}|^2 + |\mathcal{M}_{ud \rightarrow ud}|^2 + |\mathcal{M}_{u\bar{u} \rightarrow u\bar{u}}|^2 + |\mathcal{M}_{u\bar{d} \rightarrow u\bar{d}}|^2 \right) \\ & \quad \times [f_{q1} f_{q2} (1 - f_{q3})(1 - f_{q4}) - f_{q3} f_{q4} (1 - f_{q1})(1 - f_{q2})] \left. \right\} \\ & - \frac{1}{2E_1} \int \frac{d^3 p_2}{(2\pi)^3 2E_2} \frac{d^3 p_3}{(2\pi)^3 2E_3} \frac{d^3 p_4}{(2\pi)^3 2E_4} \frac{d^3 p_5}{(2\pi)^3 2E_5} \frac{d^3 p_6}{(2\pi)^3 2E_6} \\ & \quad \times (2\pi)^4 \delta^4(p_1 + p_2 + p_3 - p_4 - p_5 - p_6) \left\{ \frac{g_G^2}{4} |\mathcal{M}_{ugg \rightarrow ugg}|^2 \right. \\ & \quad \times [f_{q1} f_{g2} f_{g3} (1 - f_{q4})(1 + f_{g5})(1 + f_{g6}) - f_{q4} f_{g5} f_{g6} (1 - f_{q1})(1 + f_{g2})(1 + f_{g3})] \end{aligned}$$

$$\begin{aligned}
 & + g_Q g_G \left(\frac{1}{2} | \mathcal{M}_{uug \rightarrow uug} |^2 + | \mathcal{M}_{udg \rightarrow udg} |^2 + | \mathcal{M}_{u\bar{u}g \rightarrow u\bar{u}g} |^2 + | \mathcal{M}_{u\bar{d}g \rightarrow u\bar{d}g} |^2 \right) \\
 & \times [f_{q1} f_{q2} f_{g3} (1 - f_{q4})(1 - f_{q5})(1 + f_{g6}) - f_{q4} f_{q5} f_{g6} (1 - f_{q1})(1 - f_{q2})(1 + f_{g3})] \\
 & + g_Q^2 \left[\frac{1}{12} | \mathcal{M}_{uuu \rightarrow uuu} |^2 + \frac{1}{4} (| \mathcal{M}_{uud \rightarrow uud} |^2 + | \mathcal{M}_{udu \rightarrow udu} |^2) + \frac{1}{4} | \mathcal{M}_{udd \rightarrow udd} |^2 \right. \\
 & + \frac{1}{2} | \mathcal{M}_{u\bar{u}\bar{u} \rightarrow u\bar{u}\bar{u}} |^2 + \frac{1}{2} | \mathcal{M}_{u\bar{u}\bar{d} \rightarrow u\bar{u}\bar{d}} |^2 + | \mathcal{M}_{u\bar{d}\bar{u} \rightarrow u\bar{d}\bar{u}} |^2 + | \mathcal{M}_{u\bar{d}\bar{d} \rightarrow u\bar{d}\bar{d}} |^2 \\
 & + \frac{1}{4} | \mathcal{M}_{u\bar{u}\bar{u} \rightarrow u\bar{u}\bar{u}} |^2 + \frac{1}{2} (| \mathcal{M}_{u\bar{u}\bar{d} \rightarrow u\bar{u}\bar{d}} |^2 + | \mathcal{M}_{u\bar{d}\bar{u} \rightarrow u\bar{d}\bar{u}} |^2) + \frac{1}{4} | \mathcal{M}_{u\bar{d}\bar{d} \rightarrow u\bar{d}\bar{d}} |^2] \\
 & \left. \times [f_{q1} f_{q2} f_{q3} (1 - f_{q4})(1 - f_{q5})(1 - f_{q6}) - f_{q4} f_{q5} f_{q6} (1 - f_{q1})(1 - f_{q2})(1 - f_{q3})] \right\}, \tag{3}
 \end{aligned}$$

where \vec{v}_1 is the velocity of the massless gluon or up quark; the colour-spin degeneracy factors are $g_G = 16$ for the gluon and $g_Q = 6$ for the quark; p_1 and p_2 (p_1, p_2 and p_3) denote the four-momenta of the two (three) initial particles, and p_3 and p_4 (p_4, p_5 and p_6) of the two (three) final particles in 2-to-2 (3-to-3) scattering; and E_i is the energy component of p_i . The squared amplitudes of order α_s^2 for the elastic 2-to-2 scattering, $| \mathcal{M}_{gg \rightarrow gg} |^2$, $| \mathcal{M}_{gu \rightarrow gu} |^2$, etc., can be found in Refs. [11, 12]. The squared amplitude of order α_s^4 for the elastic ggg scattering, $| \mathcal{M}_{ggg \rightarrow ggg} |^2$, was obtained in the work of Ref. [8]. Since the elastic gluon-gluon-quark scattering involves a lot more Feynman diagrams than the elastic gqq scattering and the elastic $gq\bar{q}$ scattering, it will take two years to derive the squared amplitude for the elastic gluon-gluon-quark scattering. For the time being, we have to give up the elastic scattering of both gqq and $gq\bar{q}$, i.e. set

$$\mathcal{M}_{ugg \rightarrow ugg} = \mathcal{M}_{ggu \rightarrow ggu} = \mathcal{M}_{ggd \rightarrow ggd} = \mathcal{M}_{g\bar{g}\bar{u} \rightarrow g\bar{g}\bar{u}} = \mathcal{M}_{g\bar{g}\bar{d} \rightarrow g\bar{g}\bar{d}} = 0.$$

The squared amplitude for the elastic gluon-antiquark-antiquark scattering equals the one for the elastic gqq scattering, for example,

$$| \mathcal{M}_{g\bar{u}\bar{u} \rightarrow g\bar{u}\bar{u}} |^2 = | \mathcal{M}_{guu \rightarrow guu} |^2, \quad | \mathcal{M}_{g\bar{u}\bar{d} \rightarrow g\bar{u}\bar{d}} |^2 = | \mathcal{M}_{gud \rightarrow gud} |^2.$$

The squared amplitude $| \mathcal{M}_{qqg \rightarrow qqg} |^2$ is obtained from $| \mathcal{M}_{gqq \rightarrow gqq} |^2$ by the replacement of $p_1 \leftrightarrow p_3$ and $| \mathcal{M}_{q\bar{q}g \rightarrow q\bar{q}g} |^2$ from $| \mathcal{M}_{gq\bar{q} \rightarrow gq\bar{q}} |^2$ by the replacement of $p_1 \rightarrow p_3$, $p_2 \rightarrow p_1$ and $p_3 \rightarrow p_2$. The squared amplitudes for the elastic quark-quark-quark or antiquark-antiquark-antiquark scattering and for the elastic quark-quark-antiquark or quark-antiquark-antiquark scattering were obtained in the work of Ref. [13] and of Ref. [14], respectively. Similar equations for down quarks, up antiquarks and down antiquarks can be established.

The squared amplitude, $| \mathcal{M}_{gqq \rightarrow gqq} |^2$ for $g(p_1) + q(p_2) + q(p_3) \rightarrow g(p_4) + q(p_5) + q(p_6)$ or $| \mathcal{M}_{gq\bar{q} \rightarrow gq\bar{q}} |^2$ for $g(p_1) + q(p_2) + \bar{q}(-p_3) \rightarrow g(p_4) + q(p_5) + \bar{q}(-p_6)$, is the sum of the individually squared amplitudes of the diagrams in the three classes and interference terms of different diagrams. The sum of the two interference terms of a diagram in the first or third class and a diagram in the second class equals zero. Therefore, there is no interference between the first or third class and the second class. Any interference term between a diagram in the first class and a diagram in the third class has a very long expression and is thus not shown here. Examples of the individually squared amplitudes

are the spin- and color-summed squared amplitudes for the diagrams $D_{\sim LM}$ and $E_{\sim UU}$ which, as shown below, include the average over the spin and color states of the initial particles,

$$\begin{aligned}
 \frac{1}{8} \frac{1}{72} \sum_{\text{spins, colors}} |\mathcal{M}_{D_{\sim LM}}|^2 = & \frac{32g_s^8}{9} \frac{1}{18} (s_{12}u_{16}u_{35}^2 - s_{12}u_{16}u_{34}^2 - s_{12}u_{16}u_{26}u_{35} \\
 & + s_{12}u_{16}u_{26}u_{34} - s_{12}u_{16}^2u_{35} + s_{12}u_{16}^2u_{34} - s_{12}s_{31}u_{35}^2 \\
 & + s_{12}s_{31}u_{34}^2 + 2s_{12}s_{31}u_{26}u_{35} - s_{12}s_{31}u_{26}^2 + 2s_{12}s_{31}u_{24}u_{35} \\
 & + 2s_{12}s_{31}u_{24}u_{34} - 2s_{12}s_{31}u_{24}u_{26} - 2s_{12}s_{31}u_{16}u_{34} - 2s_{12}s_{31}u_{16}u_{24} \\
 & + s_{12}s_{31}u_{16}^2 - 2s_{12}s_{31}u_{15}u_{35} - 2s_{12}s_{31}u_{15}u_{34} + 2s_{12}s_{31}u_{15}u_{26} \\
 & + 2s_{12}s_{31}u_{15}u_{16} - s_{12}s_{31}^2u_{35} - s_{12}s_{31}^2u_{34} + s_{12}s_{31}^2u_{26} \\
 & + s_{12}s_{31}^2u_{16} + s_{12}s_{23}s_{31}u_{35} + s_{12}s_{23}s_{31}u_{34} - s_{12}s_{23}s_{31}u_{26} \\
 & - s_{12}s_{23}s_{31}u_{16} - s_{12}^2u_{16}u_{35} + s_{12}^2u_{16}u_{34} + s_{12}^2s_{31}u_{35} \\
 & - s_{12}^2s_{31}u_{34} - s_{12}^2s_{31}u_{26} - 2s_{12}^2s_{31}u_{24} + s_{12}^2s_{31}u_{16} \\
 & + 2s_{12}^2s_{31}u_{15} + s_{12}^2s_{31}^2 - s_{12}^2s_{23}s_{31}) \\
 & / [s_{12}(s_{12} + u_{16} + u_{26} - u_{34} - u_{35})(-s_{31} - s_{23} - u_{34} - u_{35})]^2, \quad (4)
 \end{aligned}$$

$$\begin{aligned}
 \frac{1}{8} \frac{1}{72} \sum_{\text{spins, colors}} |\mathcal{M}_{E_{\sim UU}}|^2 = & \frac{32g_s^8}{9} \frac{1}{18} (-s_{31}u_{15}u_{26}u_{35} + s_{31}u_{15}u_{26}^2 \\
 & + s_{31}u_{15}u_{24}u_{35} - s_{31}u_{15}u_{24}^2 - s_{31}u_{15}^2u_{26} + s_{31}u_{15}^2u_{24} - s_{31}^2u_{15}u_{26} \\
 & + s_{31}^2u_{15}u_{24} - 2s_{23}u_{15}u_{16}u_{35} + 2s_{23}u_{15}u_{16}u_{26} + 2s_{23}u_{15}u_{16}u_{24} \\
 & - s_{23}u_{15}^2u_{35} + s_{23}u_{15}^2u_{26} + s_{23}u_{15}^2u_{24} - 2s_{23}u_{15}^2u_{16} \\
 & - s_{23}u_{15}^3 - s_{23}s_{31}u_{15}u_{35} + s_{23}s_{31}u_{15}u_{26} + s_{23}s_{31}u_{15}u_{24} \\
 & - 2s_{23}s_{31}u_{15}u_{16} - 2s_{23}s_{31}u_{15}^2 - s_{23}s_{31}^2u_{15} - s_{12}s_{23}u_{15}u_{35} \\
 & + s_{12}s_{23}u_{15}u_{26} + s_{12}s_{23}u_{15}u_{24} - s_{12}s_{23}u_{15}^2 - s_{12}s_{23}s_{31}u_{15}) \\
 & / [u_{15}(s_{31} + u_{15} - u_{24} - u_{26} + u_{35})(-s_{23} - u_{24} - u_{26} + u_{15})]^2, \quad (5)
 \end{aligned}$$

where g_s is the gauge coupling constant and nine variables are defined as $s_{12} = (p_1 + p_2)^2$, $s_{23} = (p_2 + p_3)^2$, $s_{31} = (p_3 + p_1)^2$, $u_{15} = (p_1 - p_5)^2$, $u_{16} = (p_1 - p_6)^2$, $u_{24} = (p_2 - p_4)^2$, $u_{26} = (p_2 - p_6)^2$, $u_{34} = (p_3 - p_4)^2$ and $u_{35} = (p_3 - p_5)^2$. Squared amplitudes for 2-to-4 processes with two gluons and four quarks were obtained from helicity amplitudes in Ref. [15] and can also be derived from Fortran code named CompHEP [16]. One recent review on on-shell methods of scattering amplitudes in perturbative QCD has been given in Ref. [17]. Momenta of five partons among the six partons are randomly generated and the momentum of the other parton is given by energy-momentum conservation. With such a set of six momenta numerical values of the expressions in Eqs. (4) and (5) agree with numerical results of the 2-to-4 processes presented in Refs. [15, 16] by reversing the momentum of one final parton. Such agreement is also established for any other set of momenta randomly generated.

Hadronic matter and quark-gluon plasma exist below and above the critical temperature of the QCD phase transition, respectively. Due to the medium screening,

the gauge coupling constant in quark-gluon plasma is smaller than in hadronic matter and at temperatures high enough is so small that perturbative QCD can be applied. The gauge coupling constant decreases while the temperature increases [18, 19]. The higher the temperature is, the better any perturbative expansion converges. While the temperature is near the critical temperature, the perturbative expansion breaks down; but no one has determined the breakdown temperature regime.

5. Numerical solutions and discussions

Time dependence of distributions of gluons, quarks and antiquarks is determined by the transport equations which have the initial condition at $t = 0.2$ fm/ c generated by HIJING [20] for central Au-Au collisions at $\sqrt{s_{NN}} = 200$ GeV and expressed in the form [21]

$$f(k_{\perp}, y, r, z, t) = \frac{1}{16\pi R_A^2} g(k_{\perp}, y) \frac{e^{-(z-t \tanh y)^2/2\Delta_k^2}}{\sqrt{2\pi}\Delta_k}, \quad (6)$$

with

$$\Delta_k \approx \frac{2}{k_{\perp} \cosh y},$$

and

$$g(k_{\perp}, y) = \frac{(2\pi)^3}{k_{\perp} \cosh y} \frac{dN}{dy d^2k_{\perp}},$$

where R_A , k_{\perp} , y , t , z and r are the gold nucleus radius, transverse momentum, rapidity, time, coordinate in the longitudinal direction and radius in the transverse direction, respectively. The gluon and the quark have different $dN/dy d^2k_{\perp}$. One thousand and five hundred gluons within $-0.3 < z < 0.3$ fm and $r < R_A$ are created from the distribution by the rejection method. Two hundred and fifty quarks or antiquarks of the up or down flavor are created in the same region.

Scattering of two partons happens when the two partons have the closest distance less than the square root of the ratio of cross section for 2-to-2 scattering to π . The cross section for $gg \rightarrow gg$ is

$$\sigma_{gg \rightarrow gg} = \frac{g_s^4}{16\pi s^2} \frac{9}{4} \left[\frac{17s^3 + 66\mu_D^2 s(s + \mu_D^2)}{6(s + 2\mu_D^2)^2} + \frac{2s(s + 2\mu_D^2)^2}{\mu_D^2(s + \mu_D^2)} + 2(s + 2\mu_D^2) \ln \frac{\mu_D^2}{s + \mu_D^2} \right], \quad (7)$$

and the cross section for $gq \rightarrow gq$ or $g\bar{q} \rightarrow g\bar{q}$ is

$$\sigma_{gq \rightarrow gq} = \sigma_{g\bar{q} \rightarrow g\bar{q}} = \frac{g_s^4}{16\pi s^2} \left[\frac{11}{9}s + \frac{14}{9}(s + 2\mu_D^2) \ln \frac{\mu_D^2}{s + \mu_D^2} + \frac{2s(s + 2\mu_D^2)^2}{\mu_D^2(s + \mu_D^2)} \right], \quad (8)$$

where s is the square of the total energy of two colliding particles in the center-of-momentum system; μ_D is the screening mass formulated in Refs. [22, 23, 24] and is used to regularize propagators. The coupling constant $\alpha_s = g_s^2/4\pi = 0.5$ is taken in finding solutions of the transport equations. The cross section for the elastic qq , $q\bar{q}$ or $\bar{q}\bar{q}$ scattering can be found in Ref. [14] where the fraction 8/9 in Eq. (5) should be replaced by 4/9.

Scattering of three partons occurs if the three partons are in a sphere of which the center is at the center-of-mass of the three partons and of which the radius r_{hs} is [14]

$$\begin{aligned} \pi r_{\text{hs}}^2 &= \frac{1}{m} \int \frac{d^3 p_4}{(2\pi)^3 2E_4} \frac{d^3 p_5}{(2\pi)^3 2E_5} \frac{d^3 p_6}{(2\pi)^3 2E_6} \\ &\quad \times (2\pi)^4 \delta^4(p_1 + p_2 + p_3 - p_4 - p_5 - p_6) |\mathcal{M}_{3 \rightarrow 3}|^2, \end{aligned} \quad (9)$$

where $m = 1$ for $gud \rightarrow gud$, $g\bar{u}\bar{d} \rightarrow g\bar{u}\bar{d}$, $gu\bar{u} \rightarrow gu\bar{u}$, $g\bar{d}\bar{d} \rightarrow g\bar{d}\bar{d}$, $gu\bar{d} \rightarrow gu\bar{d}$ or $g\bar{d}\bar{u} \rightarrow g\bar{d}\bar{u}$, and $m = 4$ for $guu \rightarrow guu$, $g\bar{d}\bar{d} \rightarrow g\bar{d}\bar{d}$, $g\bar{u}\bar{u} \rightarrow g\bar{u}\bar{u}$ or $g\bar{d}\bar{d} \rightarrow g\bar{d}\bar{d}$.

As shown by Eq. (6), the momentum distribution in the longitudinal direction is very different from the one in the transverse direction, but gluons, quarks and antiquarks at the initial time have similar anisotropy. Gluon distribution functions in all directions overlap at the time $t = 0.68$ fm/c which corresponds to a thermalization time of the order of 0.48 fm/c and quark distribution functions at $t = 1.56$ fm/c which gives a thermalization time of about 1.36 fm/c. These distribution functions are plotted in Figs. 15 and 16, respectively. Solid curves in Figs. 15 and 16 stand for the Jüttner distribution

$$f_g(\vec{p}) = \frac{\lambda_g}{e^{|\vec{p}|/T} - \lambda_g}, \quad (10)$$

with $T = 0.5$ GeV and $\lambda_g = 0.3$ for gluon matter at $t = 0.68$ fm/c, and

$$f_q(\vec{p}) = \frac{\lambda_q}{e^{|\vec{p}|/T} + \lambda_q}, \quad (11)$$

with $T = 0.3$ GeV and $\lambda_q = 0.3$ for quark matter at $t = 1.56$ fm/c, respectively.

The solutions of the transport equations indicate that gluon matter thermalizes rapidly and quark matter thermalizes slowly. How fast thermalization is depends on squared amplitudes and distribution functions [10]. Calculations in perturbative QCD show that $|\mathcal{M}_{gu \rightarrow gu}|^2 = |\mathcal{M}_{gd \rightarrow gd}|^2 = |\mathcal{M}_{g\bar{u} \rightarrow g\bar{u}}|^2 = |\mathcal{M}_{g\bar{d} \rightarrow g\bar{d}}|^2$, then the term $g_Q(|\mathcal{M}_{gu \rightarrow gu}|^2 + |\mathcal{M}_{gd \rightarrow gd}|^2 + |\mathcal{M}_{g\bar{u} \rightarrow g\bar{u}}|^2 + |\mathcal{M}_{g\bar{d} \rightarrow g\bar{d}}|^2)$ in Eq. (2) equals $24 |\mathcal{M}_{gu \rightarrow gu}|^2$ which is near $g_G |\mathcal{M}_{ug \rightarrow ug}|^2$ in Eq. (3). Therefore, variation of the gluon distribution function caused by elastic scattering of both gq and $g\bar{q}$ is near variation of the quark distribution function caused by the same scattering. Numerical calculations lead to a similar conclusion about variation of the gluon and quark distribution functions caused by elastic scattering of gqq , $gq\bar{q}$ and $g\bar{q}\bar{q}$. Therefore, the difference between the change of gluon distribution and the change of quark distribution or the difference between the thermalization time of gluon matter and the one of quark matter is mainly given by the elastic ggg scattering and the elastic qqq scattering. Then we need to see the point of view from the ggg and qqq scattering. This is accomplished by the four aspects: (1) the gluon distribution function f_{gi} is about 2 times the quark distribution function f_{qi} ; (2) the maximum of $|\mathcal{M}_{gg \rightarrow gg}|^2 f_{gi} f_{gj}$ in Eq. (2) is an order of magnitude larger than that of $(\frac{1}{2} |\mathcal{M}_{uu \rightarrow uu}|^2 + |\mathcal{M}_{ud \rightarrow ud}|^2 + |\mathcal{M}_{u\bar{u} \rightarrow u\bar{u}}|^2 + |\mathcal{M}_{u\bar{d} \rightarrow u\bar{d}}|^2) f_{qi} f_{qj}$ in Eq. (3); (3) the maximum of $|\mathcal{M}_{ggg \rightarrow ggg}|^2$ is two orders of magnitude larger than that of $|\mathcal{M}_{qqq \rightarrow qqg}|^2$, $|\mathcal{M}_{qq\bar{q} \rightarrow qq\bar{q}}|^2$ or $|\mathcal{M}_{q\bar{q}\bar{q} \rightarrow q\bar{q}\bar{q}}|^2$; (4) the factor $g_G^2 f_{gi} f_{gj} f_{gk} / 12$ is over four times the factor $g_Q^2 f_{qi} f_{qj} f_{qk}$. Finally, we understand that the rapid thermalization

of gluon matter and the slow thermalization of quark matter result mainly from the fact that the elastic gg (ggg) scattering has a larger squared amplitude than the elastic qq or $q\bar{q}$ (qqq or $qq\bar{q}$) scattering and gluon matter is denser than quark matter.

The squared amplitude for the elastic gq (gqq or $gq\bar{q}$) scattering is comparable to the one for the elastic qq or $q\bar{q}$ (qqq or $qq\bar{q}$) scattering. To get a clear understanding of contributions of new terms of the elastic scattering of gqq and $gq\bar{q}$ in Eqs. (2) and (3), we approximate the factors, $1 + f_{gi}$ and $1 - f_{qi}$, by 1. In Eq. (2) the maximum of the new term $g_Q(|\mathcal{M}_{gu \rightarrow gu}|^2 + |\mathcal{M}_{gd \rightarrow gd}|^2 + |\mathcal{M}_{g\bar{u} \rightarrow g\bar{u}}|^2 + |\mathcal{M}_{g\bar{d} \rightarrow g\bar{d}}|^2)(f_{g1}f_{q2} - f_{g3}f_{q4})$ is about half of the maximum of the term $\frac{g_G}{2} |\mathcal{M}_{gg \rightarrow gg}|^2 (f_{g1}f_{g2} - f_{g3}f_{g4})$, and the maximum of the new term $g_Q^2[\frac{1}{4} |\mathcal{M}_{guu \rightarrow guu}|^2 + \frac{1}{2}(|\mathcal{M}_{gud \rightarrow gud}|^2 + |\mathcal{M}_{gdu \rightarrow gdu}|^2) + \frac{1}{4} |\mathcal{M}_{gdd \rightarrow gdd}|^2 + |\mathcal{M}_{gu\bar{u} \rightarrow gu\bar{u}}|^2 + |\mathcal{M}_{gud \rightarrow gu\bar{d}}|^2 + |\mathcal{M}_{gd\bar{u} \rightarrow gd\bar{u}}|^2 + |\mathcal{M}_{g\bar{d}\bar{d} \rightarrow g\bar{d}\bar{d}}|^2 + \frac{1}{4} |\mathcal{M}_{g\bar{u}\bar{u} \rightarrow g\bar{u}\bar{u}}|^2 + \frac{1}{2}(|\mathcal{M}_{g\bar{u}\bar{d} \rightarrow g\bar{u}\bar{d}}|^2 + |\mathcal{M}_{g\bar{d}\bar{u} \rightarrow g\bar{d}\bar{u}}|^2) + \frac{1}{4} |\mathcal{M}_{g\bar{d}\bar{d} \rightarrow g\bar{d}\bar{d}}|^2](f_{g1}f_{q2}f_{q3} - f_{g4}f_{q5}f_{q6})$ is about one-fifth of the maximum of $\frac{g_G^2}{12} |\mathcal{M}_{ggg \rightarrow ggg}|^2 (f_{g1}f_{g2}f_{g3} - f_{g4}f_{g5}f_{g6})$. Therefore, the new terms provide small contributions to thermalization of gluon matter. In Eq. (3) the maximum of the new term $g_G |\mathcal{M}_{ug \rightarrow ug}|^2 (f_{q1}f_{q2} - f_{q3}f_{q4})$ is about 2 times the maximum of the term $g_Q(\frac{1}{2} |\mathcal{M}_{uu \rightarrow uu}|^2 + |\mathcal{M}_{ud \rightarrow ud}|^2 + |\mathcal{M}_{u\bar{u} \rightarrow u\bar{u}}|^2 + |\mathcal{M}_{u\bar{d} \rightarrow u\bar{d}}|^2)(f_{q1}f_{q2} - f_{q3}f_{q4})$, and the maximum of the new term $g_Q g_G(\frac{1}{2} |\mathcal{M}_{uug \rightarrow uug}|^2 + |\mathcal{M}_{udg \rightarrow udg}|^2 + |\mathcal{M}_{u\bar{u}g \rightarrow u\bar{u}g}|^2 + |\mathcal{M}_{u\bar{d}g \rightarrow u\bar{d}g}|^2)(f_{q1}f_{q2}f_{q3} - f_{q4}f_{q5}f_{q6})$ is near the maximum of $g_Q^2[\frac{1}{12} |\mathcal{M}_{uuu \rightarrow uuu}|^2 + \frac{1}{4}(|\mathcal{M}_{uud \rightarrow uud}|^2 + |\mathcal{M}_{udu \rightarrow udu}|^2) + \frac{1}{4} |\mathcal{M}_{udd \rightarrow udd}|^2 + \frac{1}{2} |\mathcal{M}_{uu\bar{u} \rightarrow uu\bar{u}}|^2 + \frac{1}{2} |\mathcal{M}_{uud \rightarrow u\bar{u}\bar{d}}|^2 + |\mathcal{M}_{ud\bar{u} \rightarrow ud\bar{u}}|^2 + |\mathcal{M}_{udd \rightarrow u\bar{d}\bar{d}}|^2 + \frac{1}{4} |\mathcal{M}_{u\bar{u}\bar{u} \rightarrow u\bar{u}\bar{u}}|^2 + \frac{1}{2}(|\mathcal{M}_{u\bar{u}\bar{d} \rightarrow u\bar{u}\bar{d}}|^2 + |\mathcal{M}_{u\bar{d}\bar{u} \rightarrow u\bar{d}\bar{u}}|^2) + \frac{1}{4} |\mathcal{M}_{u\bar{d}\bar{d} \rightarrow u\bar{d}\bar{d}}|^2](f_{q1}f_{q2}f_{q3} - f_{q4}f_{q5}f_{q6})$. Hence, the new terms have comparable contributions to thermalization of quark matter. Governed by the elastic scattering of qq , $q\bar{q}$, qqq , $qq\bar{q}$ and $q\bar{q}\bar{q}$, a thermalization time of the order of 1.55 fm/ c was obtained in Ref. [14] for quark matter with the same initial distribution as Eq. (6). Hence, the elastic scattering of gq , gqq and $gq\bar{q}$ shortens the thermalization time of quark matter by the amount 0.19 fm/ c . About half of the amount is a consequence of the elastic gqq and $gq\bar{q}$ scattering. The elastic gq scattering, the elastic gqq scattering and the elastic $gq\bar{q}$ scattering have different contributions in shortening the thermalization time. Taking up-quark matter as an example, amounts by which the thermalization time is shortened by relevant elastic scattering are listed in Table 1. The amount by which the thermalization time is shortened by the elastic $gq\bar{q}$ scattering is larger than by gqq .

In Ref. [8] one thousand gluons are generated from a distribution that is homogeneous in coordinate space but anisotropic in momentum space. Gluon matter is controlled to evolve in the longitudinal direction and is governed by the elastic ggg scattering. The resultant fugacity and temperature are 0.065 and 0.75 GeV, respectively. In Ref. [13] six hundred and sixty-six quarks are generated from a distribution similar to that in Ref. [8]. Quark matter is also controlled to evolve in the longitudinal direction and is governed by the elastic qqq scattering. The resultant fugacity and temperature are 0.04 and 0.59 GeV, respectively. Due to the restriction of longitudinal expansion, the two fugacities are small and the two temperatures are high. In Ref. [14] five hundred quarks and five hundred antiquarks are created from the same distribution as that in

Eq. (6). Governed by the elastic scattering of qqq , $qq\bar{q}$, $q\bar{q}\bar{q}$ and $\bar{q}\bar{q}\bar{q}$, quark matter and antiquark matter evolve in both the transverse direction and the longitudinal direction. The resultant fugacity and temperature are 0.31 and 0.27 GeV, respectively. Without the restriction of longitudinal expansion, the fugacities in Ref. [14] and in the present work are not small and the temperatures are not higher than those in Refs. [8] and [13]. The fugacity and temperature obtained in the present work must be different from those in Ref. [14] since the present work involves gluon matter that is absent in Ref. [14].

Even though the study and application of elastic 4-to-4 scattering is not the purpose of the present work, we still can know the occurrence probability of the 4-parton scattering and it has been shown in Ref. [14]. One thousand and five hundred partons were generated from the same distribution as that in Eq. (6) within $-0.3 \text{ fm} < z < 0.3 \text{ fm}$ and $r < R_A$. Given an interaction range of 0.62 fm, the 2-parton scattering has the occurrence probability of 30%, the 3-parton scattering 20%, and the 4-parton scattering 14.6%. Therefore, the elastic 4-parton scattering is expected to give a smaller contribution to thermalization than the elastic 3-parton scattering. Interaction of partons in a sphere with a radius the same as the interaction range takes place and the number of partons in such a sphere is at most 14. This means that at most 14-parton scattering is allowed. As a consequence, the occurrence probability of 15-parton scattering is zero and the one of the 14-parton scattering is very small. The occurrence probabilities for 5-parton, 6-parton, 7-parton, 8-parton, 9-parton, 10-parton and 11-parton scattering are 11%, 9%, 7.5%, 4.4%, 2.3%, 0.9% and 0.2%, respectively. The occurrence probabilities for 12-parton scattering and 13-parton scattering are negligible. The sum of the occurrence probabilities from the 2-parton scattering through the 14-parton scattering equals 1 and the occurrence probabilities form a convergent series.

6. Summary

We have established the transport equations that include the squared amplitudes for the elastic scattering of gqq , $gq\bar{q}$ and $g\bar{q}\bar{q}$. The squared amplitudes are derived at the tree level of the scattering in perturbative QCD and are expressed in terms of the nine Lorentz-invariant momentum variables. The elastic scattering of gqq , $gq\bar{q}$ and $g\bar{q}\bar{q}$ shortens the thermalization time of quark matter as well as antiquark matter. This is an effect of the three-body scattering while the number density is high. In not only quark-gluon matter with a high number density but also a very dense scalar field system, the elastic 3-to-3 scattering plays a significant role [25].

Acknowledgments

This work was supported in part by the National Natural Science Foundation of China under Grant No. 10675079 and in part by Shanghai Leading Academic Discipline Project (project number S30105).

References

- [1] Shuryak E 1992 *Phys. Rev. Lett.* **68** 3270
- [2] Geiger K 1992 *Phys. Rev.* **D46** 4965
Geiger K 1992 *Phys. Rev.* **D46** 4986
- [3] Biró T S, van Doorn E, Müller B, Thoma M H and Wang X.-N. 1993 *Phys. Rev.* **C48** 1275
- [4] Wong S M H 1996 *Phys. Rev.* **C54** 2588
- [5] Nayak G C, Dumitru A, McLerran L and Greiner W 2001 *Nucl. Phys.* **A687** 457
- [6] Shin G R and Müller B 2003 *J. Phys.* **G29** 2485
- [7] Xu Z and Greiner C 2005 *Phys. Rev.* **C71** 064901
- [8] Xu X.-M., Sun Y, Chen A.-Q. and Zheng L 2004 *Nucl. Phys.* **A744** 347
- [9] Liu W and Ko C M 2006 *Preprint* nucl-th/0603004
Liu W and Ko C M 2007 *J. Phys.* **G34** S775
- [10] Xu X.-M. 2007 *J. Phys.* **G34** S859
- [11] Cutler R and Sivers D 1978 *Phys. Rev.* **D17** 196
- [12] Combridge B L, Kripfganz J and Ranft J 1977 *Phys. Lett.* **B70** 234
- [13] Xu X.-M., Peng R and Weber H J 2005 *Phys. Lett.* **B629** 68
- [14] Xu X.-M., Ma C.-C., Chen A.-Q. and Weber H J 2007 *Phys. Lett.* **B645** 146
- [15] Gunion J F and Kunszt Z 1985 *Phys. Lett.* **B159** 167
Gunion J F and Kunszt Z 1986 *Phys. Lett.* **B176** 477
- [16] Pukhov A, et al. 2000 *Preprint* hep-ph/9908288v2
- [17] Bern Z, Dixon L J and Kosower D A 2007 *Ann. Phys.* **322** 1587
- [18] Kapusta J I 2007 *J. Phys.* **G34** S295
- [19] Laine M and Schröder Y 2005 *JHEP* **03** 067
- [20] Wang X.-N. and Gyulassy M 1991 *Phys. Rev.* **D44** 3501
Gyulassy M and Wang X.-N. 1994 *Comput. Phys. Commun.* **83** 307
Wang X.-N. 1997 *Phys. Rep.* **280** 287
- [21] Lévai P, Müller B and Wang X.-N. 1995 *Phys. Rev.* **C51** 3326
- [22] Biró T S, Müller B and Wang X.-N. 1992 *Phys. Lett.* **B283** 171
- [23] Bass S A, Müller B and Srivastava D K 2003 *Phys. Lett.* **B551** 277
- [24] Kalashnikov O K and Klimov V V 1980 *Sov. J. Nucl. Phys.* **31** 699
Kalashnikov O K and Klimov V V 1980 *Yad. Fiz.* **31** 1357
Klimov V V 1982 *Sov. Phys. JETP* **55** 199
Klimov V V 1982 *Zh. Eksp. Teor. Fiz.* **82** 336
- [25] Carrington M E and Mrówczyński S 2005 *Phys. Rev.* **D71** 065007

Table 1. Amounts by which the thermalization time is shortened.

$gu \rightarrow gu$	$guu \rightarrow guu, gud \rightarrow gud$	$gu\bar{u} \rightarrow gu\bar{u}, gud\bar{d} \rightarrow gud\bar{d}$
0.091 fm/ c	0.046 fm/ c	0.053 fm/ c

Thermalization of quark-gluon matter with the elastic scattering of gqq , $gq\bar{q}$ and $g\bar{q}\bar{q}$ 14

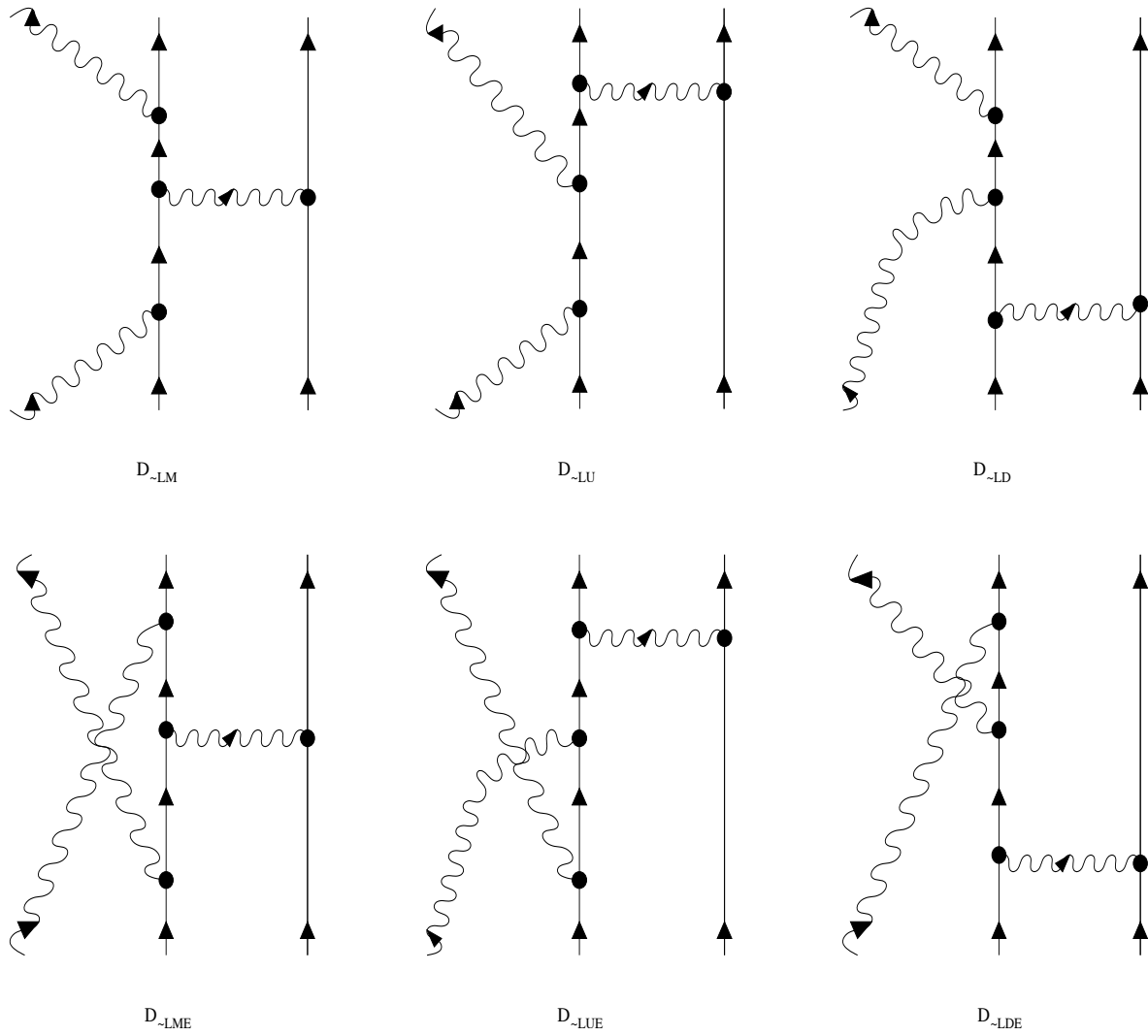


Figure 1. Elastic gluon-quark-quark scattering.

Thermalization of quark-gluon matter with the elastic scattering of gqq , $gq\bar{q}$ and $g\bar{q}\bar{q}$ 15

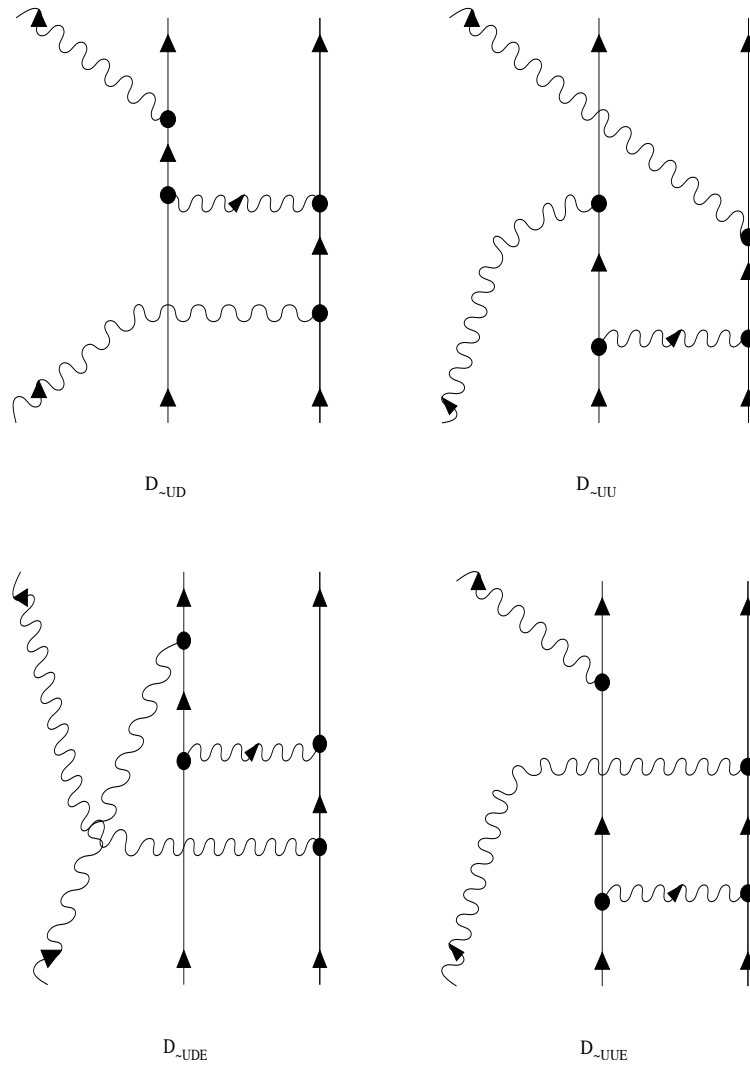


Figure 2. Elastic gluon-quark-quark scattering.

Thermalization of quark-gluon matter with the elastic scattering of gqq , $gq\bar{q}$ and $g\bar{q}\bar{q}$ 16

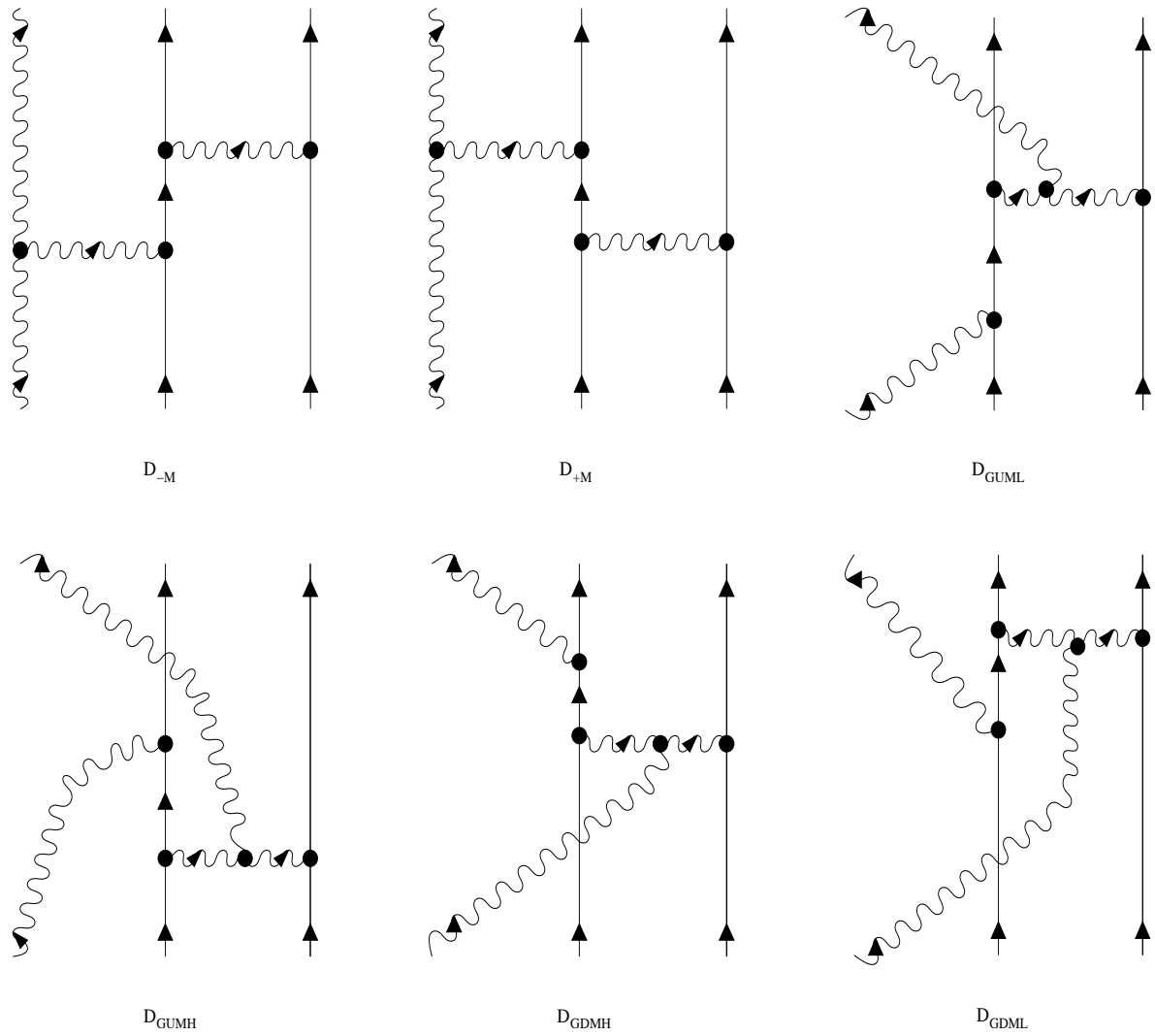


Figure 3. Elastic gluon-quark-quark scattering.

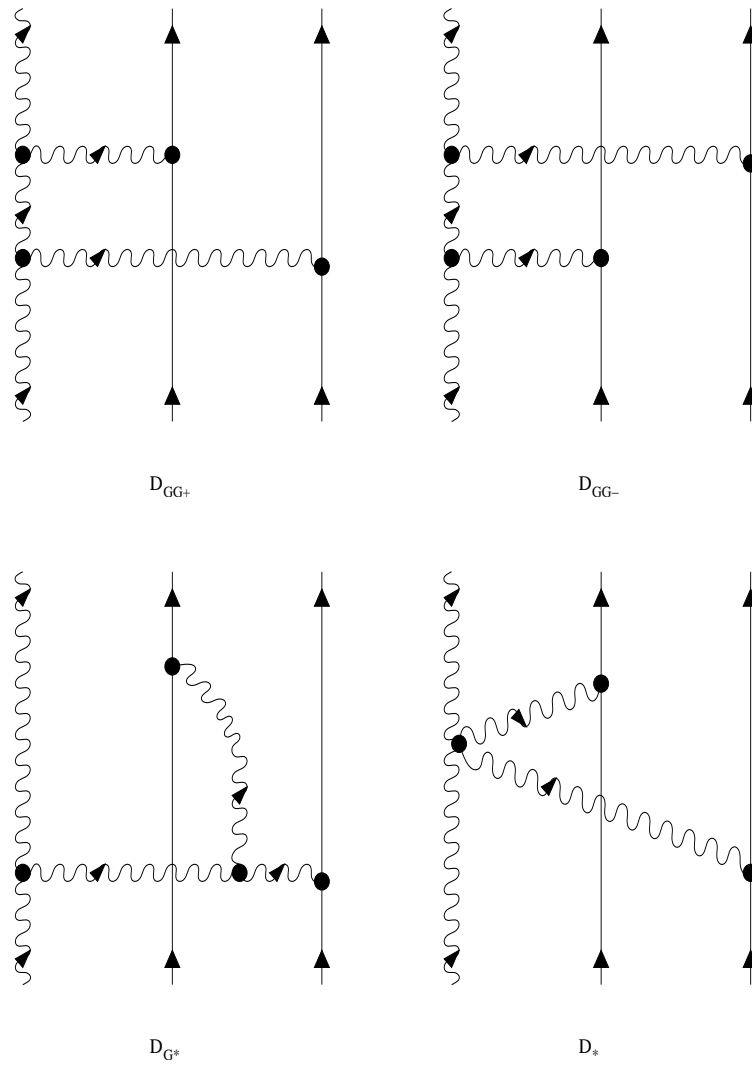


Figure 4. Elastic gluon-quark-quark scattering.

Thermalization of quark-gluon matter with the elastic scattering of gqq , $gq\bar{q}$ and $g\bar{q}\bar{q}$ 18

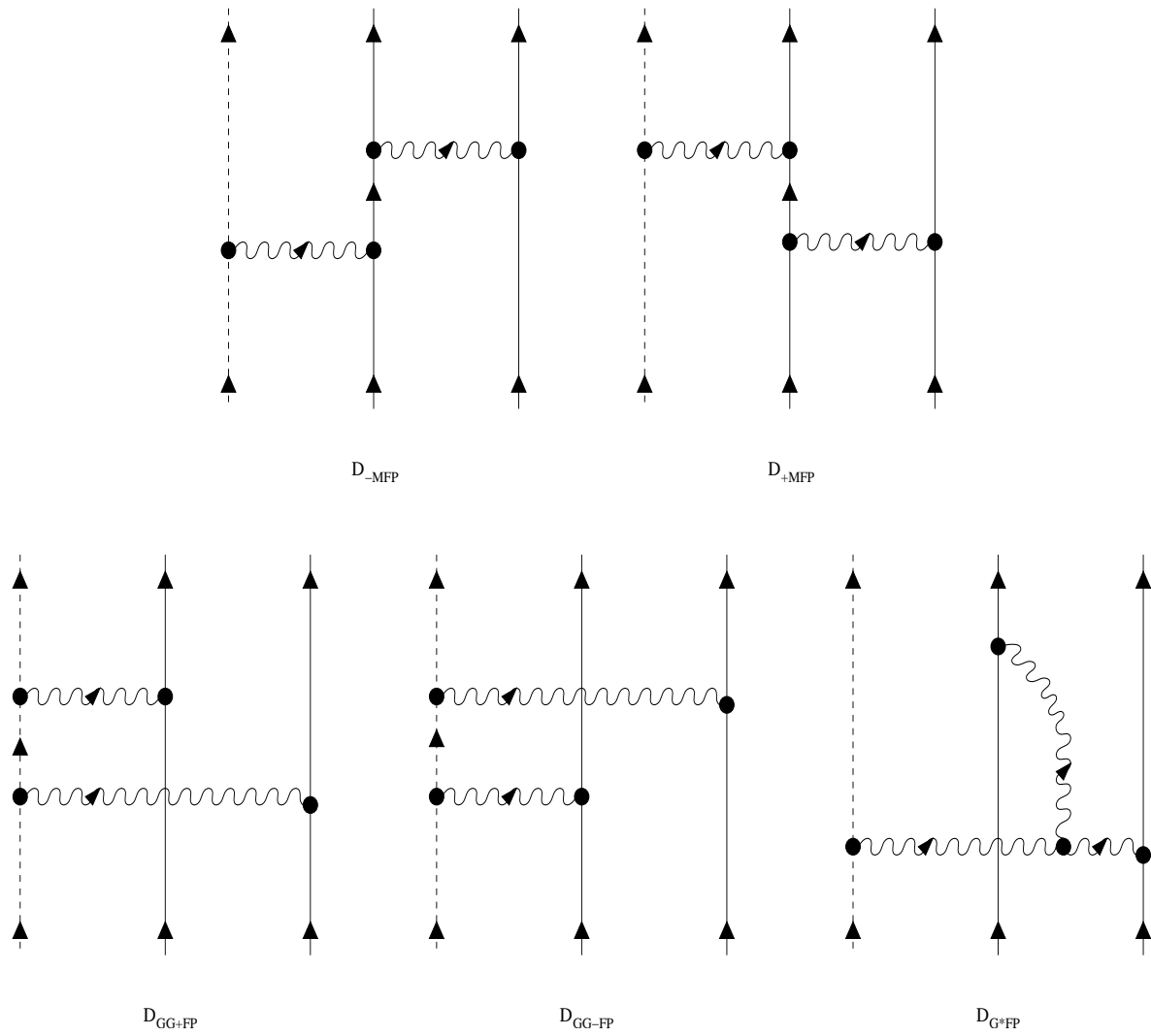


Figure 5. Elastic ghost-quark-quark scattering.

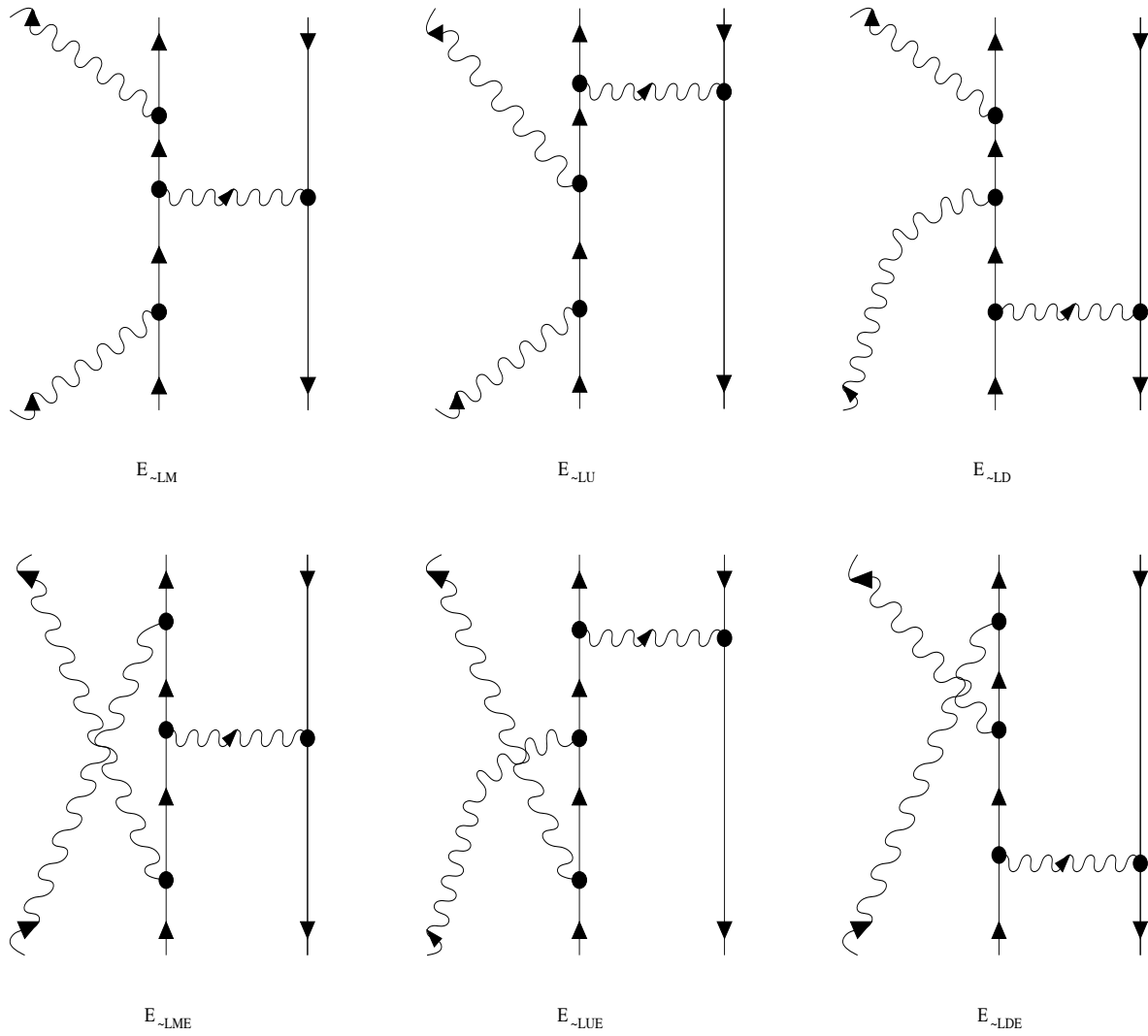


Figure 6. Elastic gluon-quark-antiquark scattering.

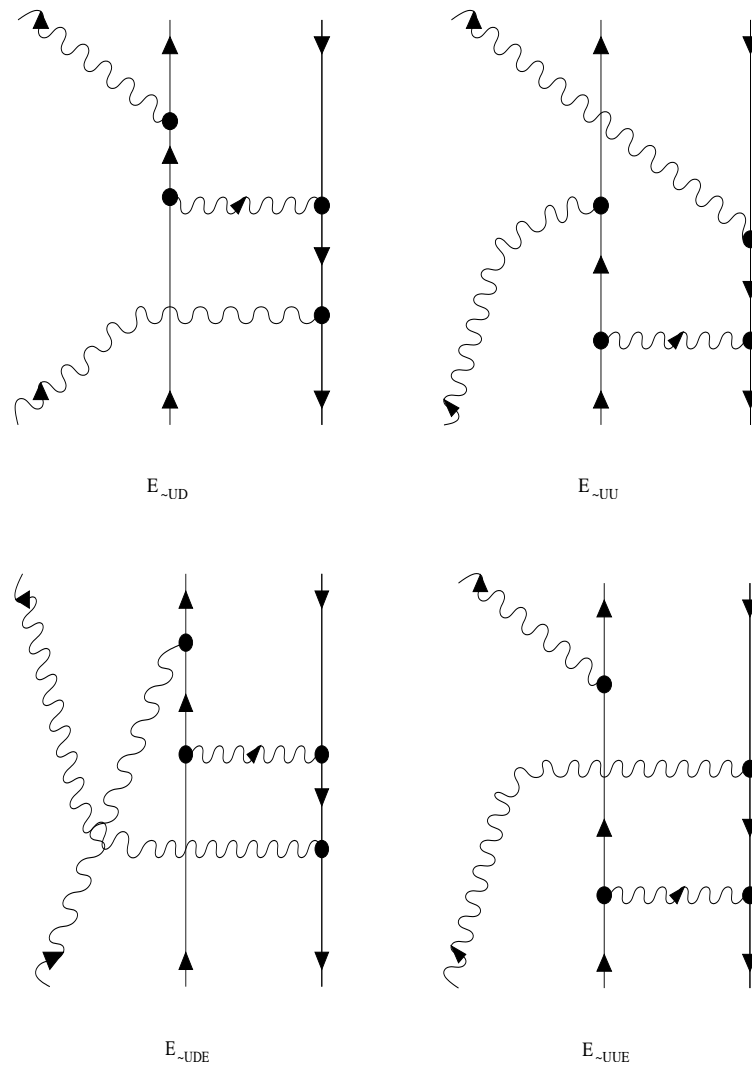


Figure 7. Elastic gluon-quark-antiquark scattering.

Thermalization of quark-gluon matter with the elastic scattering of gqq , $gq\bar{q}$ and $g\bar{q}\bar{q}$ 21

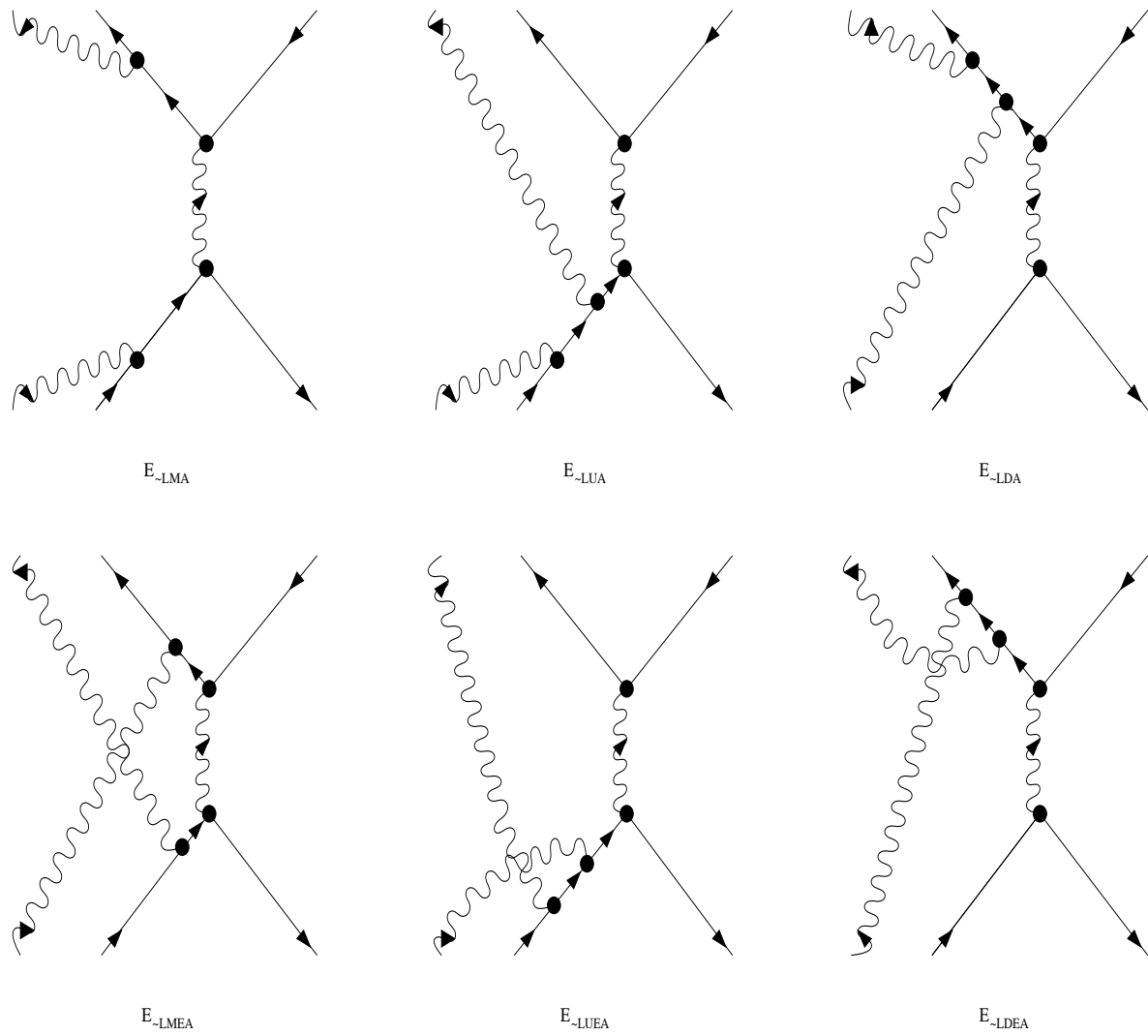


Figure 8. Elastic gluon-quark-antiquark scattering.

Thermalization of quark-gluon matter with the elastic scattering of gqq , $gq\bar{q}$ and $g\bar{q}\bar{q}$ 22

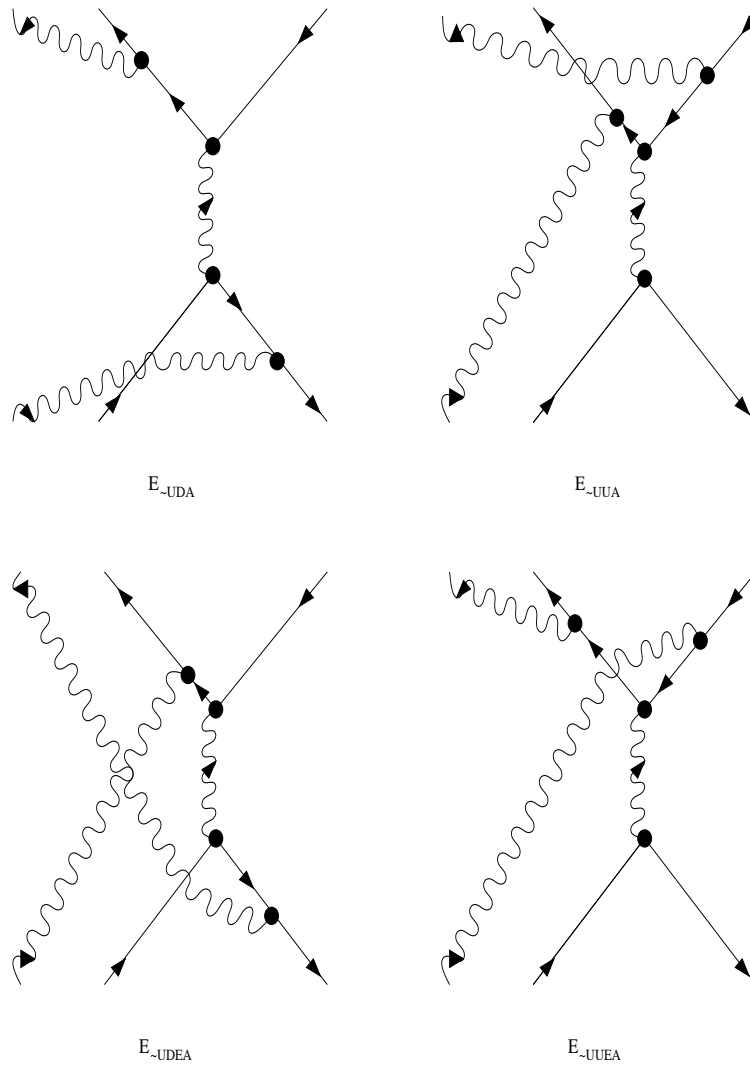


Figure 9. Elastic gluon-quark-antiquark scattering.

Thermalization of quark-gluon matter with the elastic scattering of gqq , $gq\bar{q}$ and $g\bar{q}\bar{q}$ 23

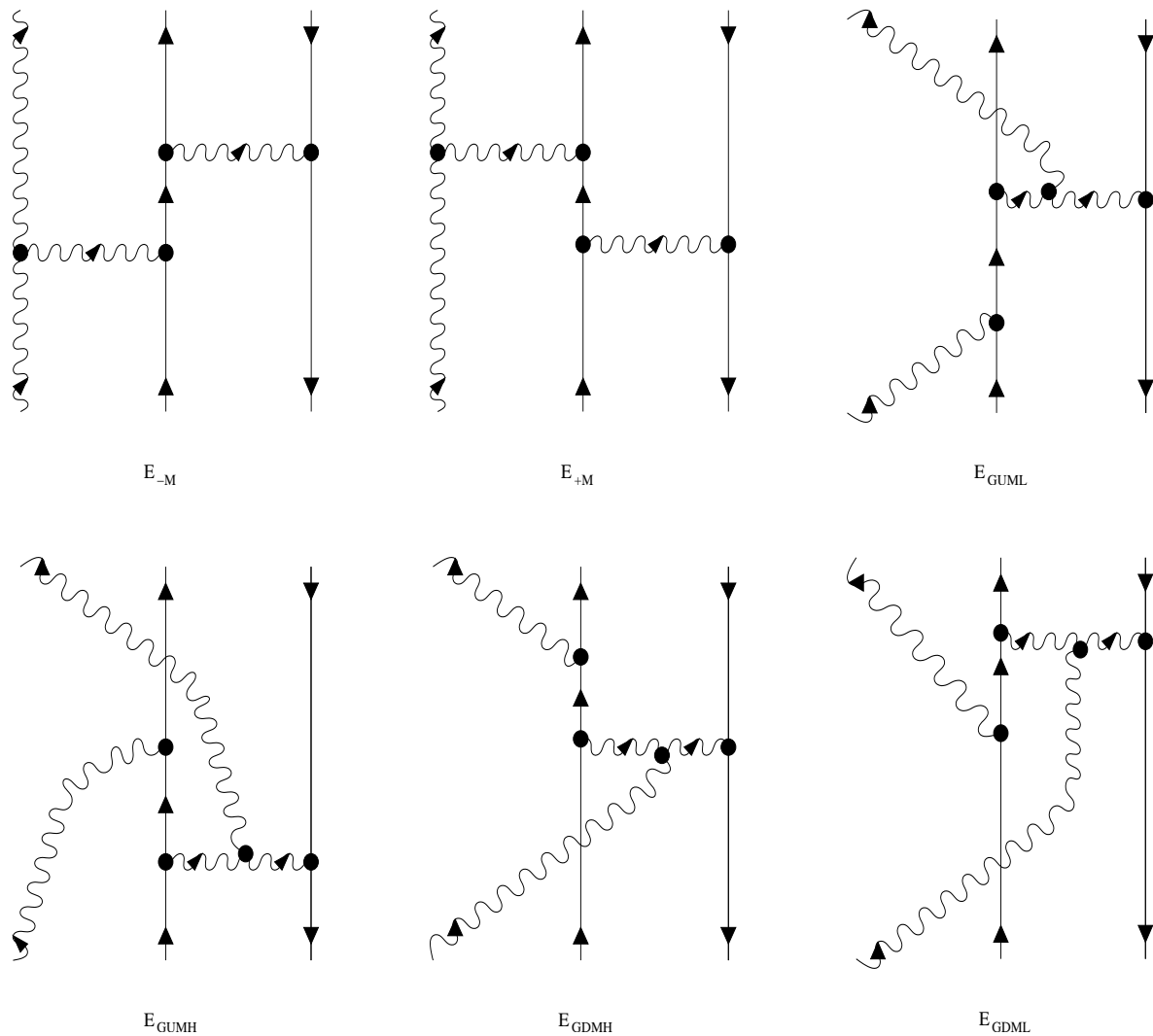


Figure 10. Elastic gluon-quark-antiquark scattering.

Thermalization of quark-gluon matter with the elastic scattering of gqq , $gq\bar{q}$ and $g\bar{q}\bar{q}$ 24

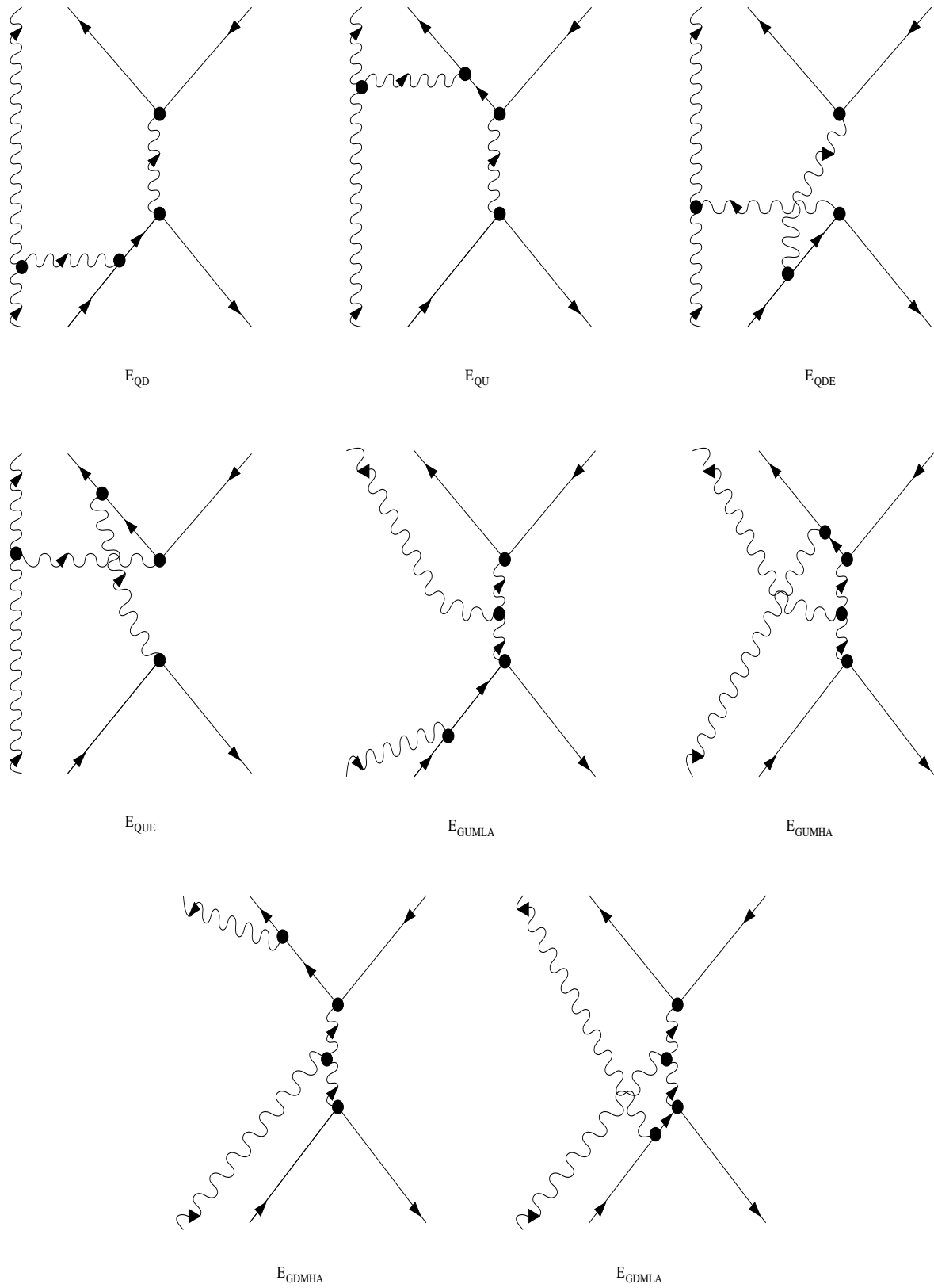


Figure 11. Elastic gluon-quark-antiquark scattering.

Thermalization of quark-gluon matter with the elastic scattering of gqq , $gq\bar{q}$ and $g\bar{q}\bar{q}$ 25

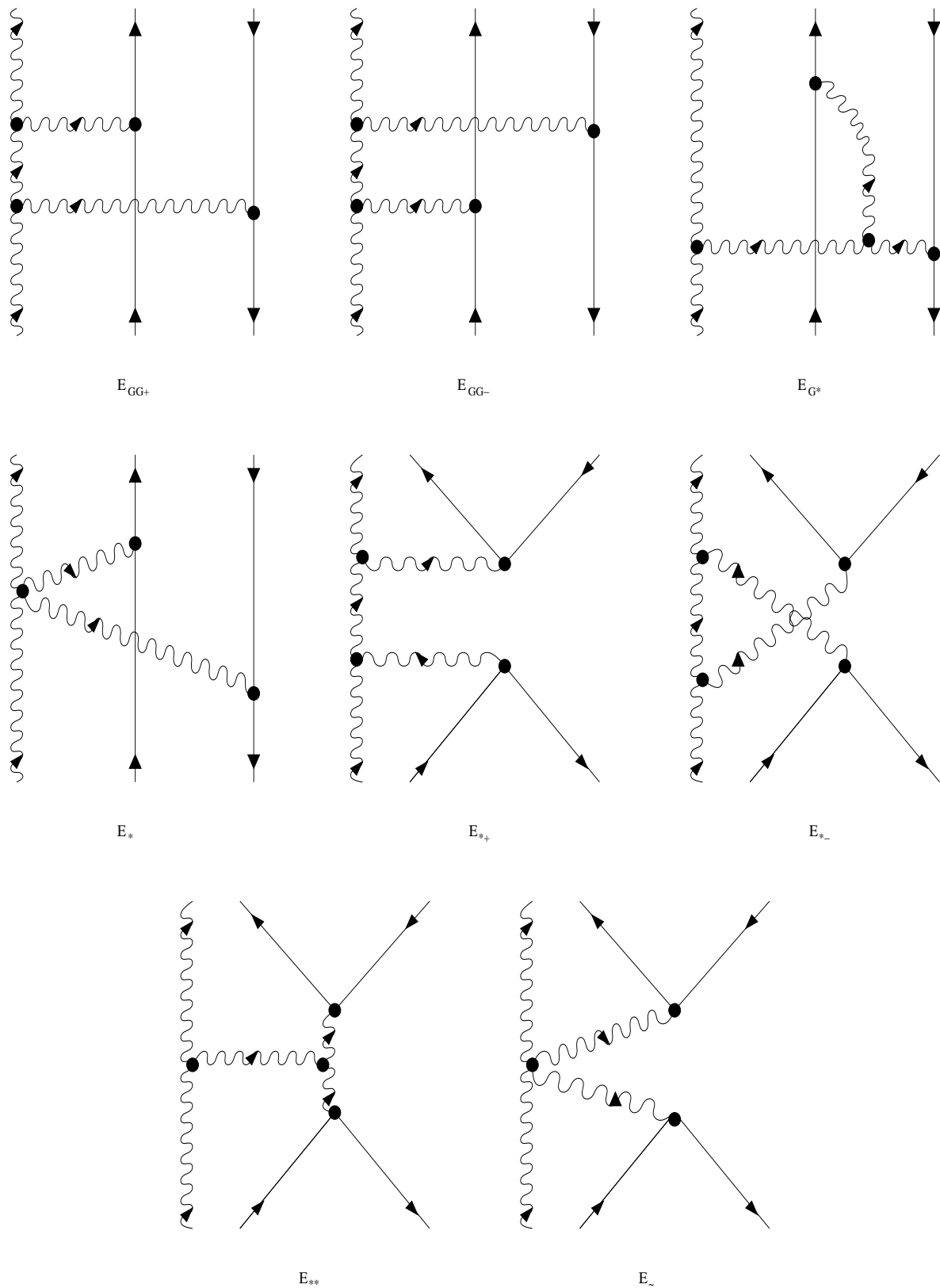


Figure 12. Elastic gluon-quark-antiquark scattering.

Thermalization of quark-gluon matter with the elastic scattering of gqq , $gq\bar{q}$ and $g\bar{q}\bar{q}$ 26

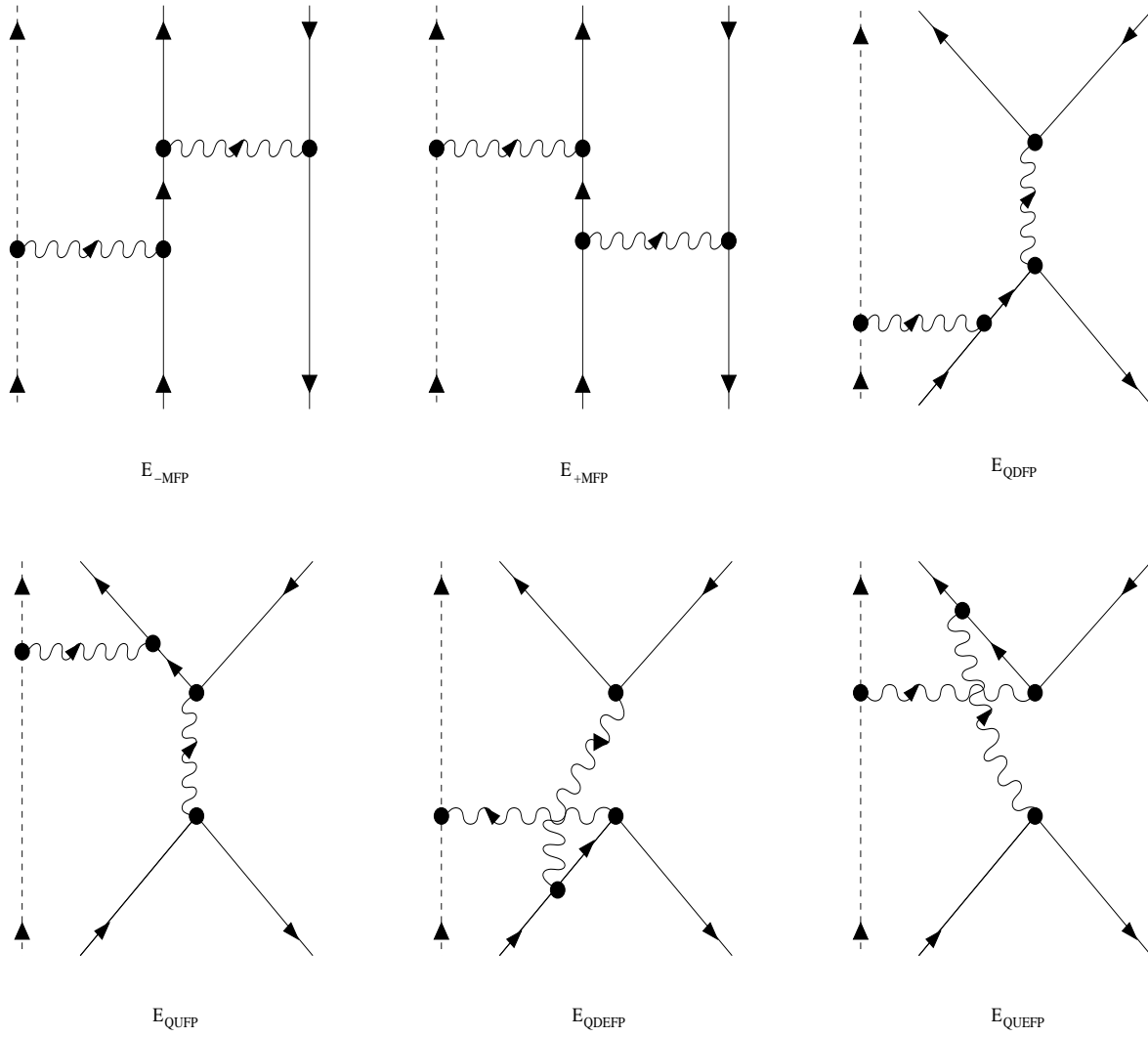


Figure 13. Elastic ghost-quark-antiquark scattering.

Thermalization of quark-gluon matter with the elastic scattering of gqq , $gq\bar{q}$ and $g\bar{q}\bar{q}$ 27

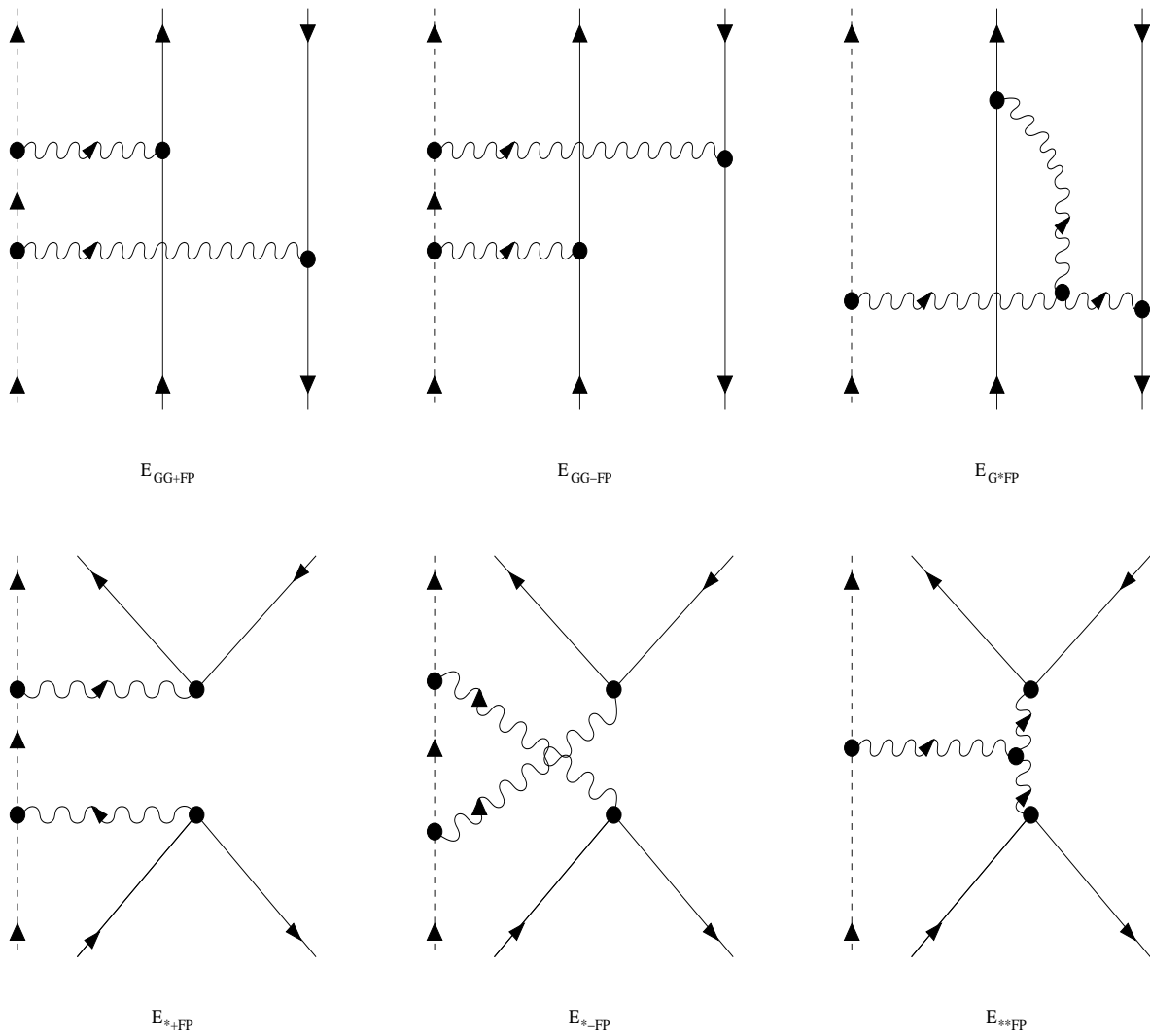


Figure 14. Elastic ghost-quark-antiquark scattering.

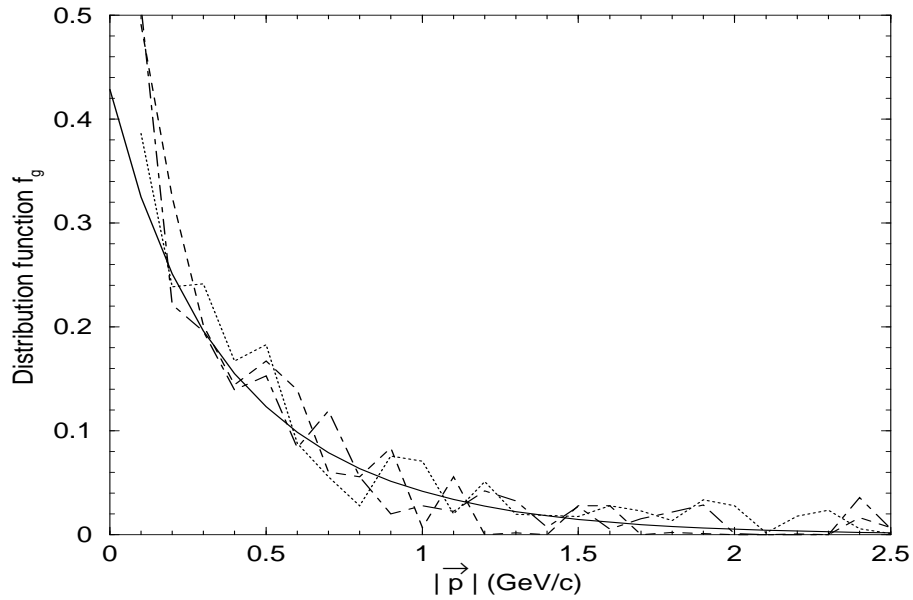


Figure 15. Gluon distribution functions versus momentum in different directions while gluon matter arrives at thermal equilibrium. The dotted, dashed and dot-dashed curves correspond to the angles relative to one incoming beam direction $\theta = 0^\circ, 45^\circ, 90^\circ$, respectively. The solid curve represents the thermal distribution function.

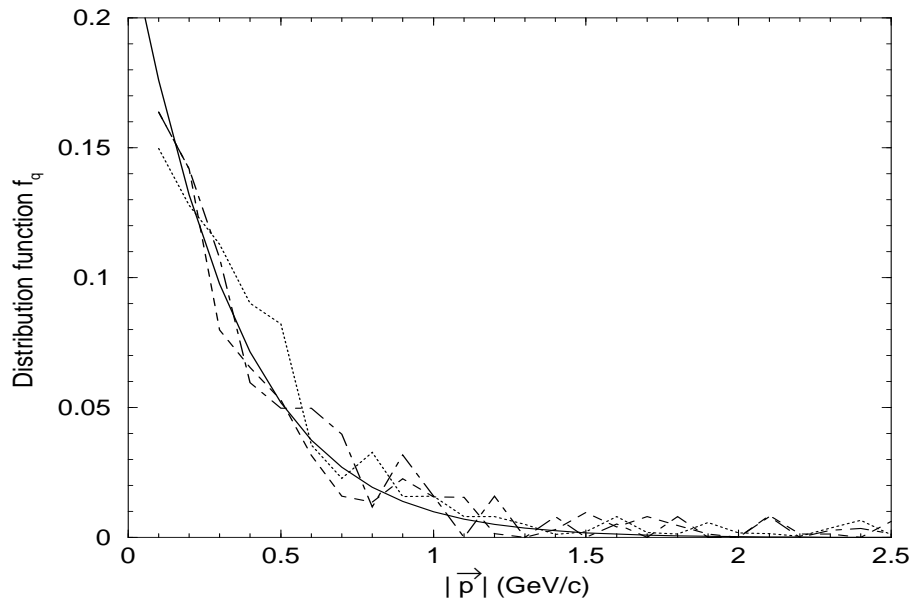


Figure 16. The same as Fig. 15, except for quark distribution functions while quark matter arrives at thermal equilibrium.